MR imaging-guided biliary drainage in an open low-field system: First clinical experiences

F. K. Wacker[1], S. Faiss[2], K. Reither[1], T. Zimmer[2], M. Wendt[3,4], K.-J. Wolf[1]

[1] Department of Radiology
[2] Department of Internal Medicine – Gastroenterology, University Hospital Benjamin Franklin, Free University of Berlin, Germany
[3] Department of Radiology, Hospitals of Cleveland, Case Western Reserve University, Ohio, USA
[4] Siemens Medical Systems, Iselin, NJ, USA

Purpose: To test the feasibility of MR imaging (MRI)-guided percutaneous biliary drainages in patients using an open MR-system. **Methods:** 6 patients with mechanical cholestasis underwent MRI-guided puncture and catheterization of the biliary system following intervention planning with magnetic resonance cholangiography (MRC) in an open low-field MR system. Data on the number of punctures required, success in establishing external and internal drainage, and total procedure time were compared to those of 6 patients who underwent biliary drainage with fluoroscopic guidance. **Results:** MRC facilitated intervention planning in all patients. Near-real-time MR imaging enabled interactive positioning of the devices. The bile ducts were punctured under MRI control in three patients in the first, in two in the second, and in one in the third attempt. MRI-guided puncture was faster than the fluoroscopic procedure. Catheterization for external drainage was successful in all patients. Passing the obstructions was not possible under MRI guidance. The procedure time for MRI-guided catheterization was longer than in the conventional technique. **Conclusion:** MRI-guidance allows reliable placement of an external biliary drainage in an open low-field MR system.

Key words: MR imaging-guided procedures – interventional MRI – MR cholangiography – biliary drainage – susceptibility artifacts

Introduction

Most reports about MRI-guided interventions in patients in open MR systems have thus far been limited to biopsies [1,2,3] and the monitoring of ablative techniques [4,5,6], where MRI either replaces or supplements another tomographic procedure. Reports on complex MRI-guided interventions have so far primarily dealt with animal experiments [7,8]. A few technical reports are available on catheter manipulation in a volunteer [9] as well as on stent placement [10].

Percutaneous biliary drainage in patients with mechanical cholestasis is usually done under fluoroscopic control when endoscopic treatment has failed or cannot be carried out due to the anatomic situation. A disadvantage of fluoroscopic control is that the biliary tree is invisible on fluoroscopy until the biliary tree is accessed and filled with contrast. Puncture is thus done under blind condition requiring multiple passes and causing additional trauma. Magnetic resonance cholangiography (MRC) can be helpful in this situation, because it allows reliable identification and localization of biliary strictures and obstructions prior to the intervention [11]. Based on diagnostic MRC, MRI can be used in the same session for puncture guidance with permanent bile duct visualization when an open MR-scanner is available [7,8]. This method has already been proven suitable in animal experiments using fast T_2-weighted imaging combined with susceptibility-based MR visualization [8], which exploit the local magnetic field inhomogeneities generated by the intervention devices, causing them to appear as a signal loss in the MR image [8,9,12].

The aim of this pilot study was to test the feasibility of MRI-guided percutaneous biliary drainage in patients, using susceptibility-based device visualization.

Materials and Methods

Patient

Twelve patients with mechanical cholestasis due to malignant stenoses (9 men, 3 women with an average age of 72 years) underwent percutaneous transhepatic biliary drainage procedures. One to 3 days prior to percutaneous intervention, an unsuccessful attempt was made at endoscopic drainage. In 6 patients the drainage was placed under MRI guidance; 6 patients underwent conventional biliary drainage under fluoroscopic control with the usual technique [13]. Thus comparative data were obtained on procedure time, number of punctures required, success in establishing drainage, and acceptance of the procedures. Patients were randomly assigned to one of the two groups. The study protocol was approved by the institutional review board. One day prior to intervention the patients gave their written informed consent. All interventions were performed by an interventional radiologist (FKW) in association with an gastroenterologist (SF).

MRI-guided interventions

The patients were placed in a supine position in an open-configuration whole-body MRI system at 0.2 Tesla (Magnetom Open, Siemens, Erlangen). Four patients were positioned with the right side of the body toward the device opening; 2 patients with the left side toward the opening. After generating a localizer, a T_1-weighted gradient echo sequence (FLASH, repetition time (TR) 220 ms, echo time (TE) 9 ms, flip angle 80°, 128 ×

Fortschr Röntgenstr 2000; 172: 744 – 747

ISSN 1438 – 9029

256 matrix, 8 mm slice thickness, 10 slices, 1 acquisition, 23 s measurement time) was acquired in the axial plane using the breath-hold technique. The planning of the MR-guided interventions was aided by MRC images, which were acquired in the axial, coronal, and coronal oblique planes. With 5 s acquisition time, the heavily T_2 -weighted RARE sequence (effective TE: 1100 ms, echo interval 11.64 ms, 240 × 256 matrix, echo train 240, 100 mm slice thickness) delivered projection images of the dilated biliary system (Fig. **1 a**). Based on these images, the optimal percutaneous access route was planned on the monitor and visualized with a T_2-weighted true FISP sequence (TR 12.5 ms, TE 5.9 ms, flip angle 80°, 128 × 256 matrix, 8 mm slice thickness, 1 acquisition). Depending on the position and course of the bile duct to be punctured, either the axial (n = 3), axial oblique (n = 1), or coronal (n = 2) orientation was selected for image control of the puncture. During continuous image acquisition with an image update every 1.3 seconds, the puncture point was located with a water-filled syringe. If puncture was not possible in the initially selected plane, adjacent slices were acquired or the slice orientation was changed.

Prior to beginning the intervention, an antibiosis containing ceftriaxone (2 g i. v., Rocephin®, Hoffmann-LaRoche, Grenzach) was administered. MRI-guided percutaneous transhepatic puncture and drainage were performed under local anesthesia (10 ml lidocaine hydrochloride, B. Braun, Melsungen) and sedation (2 – 5 mg midazolam i. v., Dormicum®, Hoffmann-LaRoche, Grenzach). In the first step a needle (18 G diameter, Somatex, Berlin), passively visible in the MR images, was advanced in the selected bile duct under continuous MRI guidance using the true FISP sequence. Because the open MRI was equipped with an additional control console (In-Room MR Console, Siemens, Erlangen) in the magnet room, image viewing and device guidance were possible while sitting next to the patient. Successful MRI-guided puncture either led to a spontaneous bile reflux or enabled bile aspiration. Subsequently we injected diluted paramagnetic contrast agent (Gd-DTPA, 2 mmol/l, Magnevist®, Schering, Berlin) into the bile ducts. Following injection, a T_1-weighted gradient echo sequence was applied for monitoring (Fig. **1 b**); FLASH: TR 110 ms, TE 9 ms, flip angle 80°, 128 × 256 matrix, 8 mm slice thickness, 5 slices, 1 acquisition, 13 s measurement time). After documentation, a guide wire of 0.035 inches in diameter was advanced through the needle. We used a wire (prototype, Somatex, Berlin) made of nitinol that induced no artifacts; however, it has a short ferromagnetic case on its tipp that causes a susceptibility artifact. Through the guide wire we inserted a catheter (prototype, Somatex, Berlin) that was completely visible in the MR image due to its magnetite content. The catheter was advanced

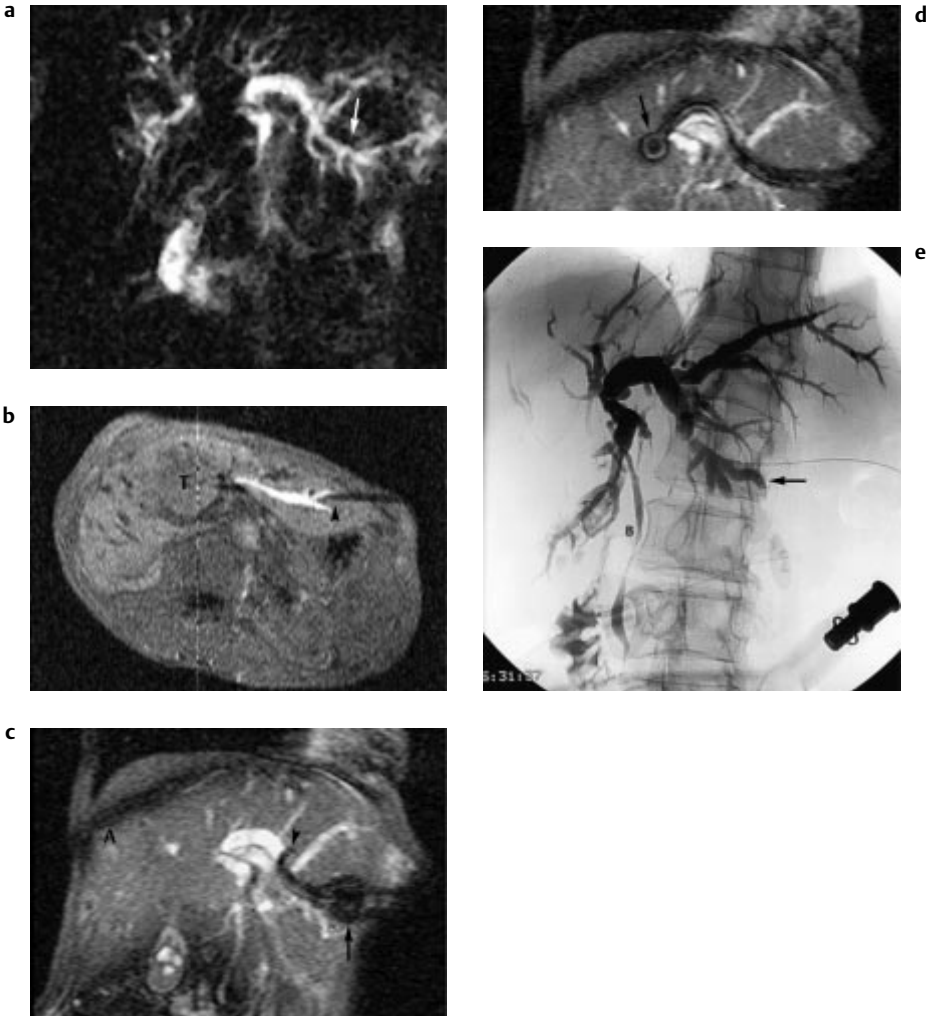

Fig. 1 Cholestasis patient with a central metastasis of a colorectal carcinoma: (**a**) The oblique coronal MR cholangiography facilitates the determination of the optimal access route for a percutaneous puncture of the dilated bile ducts in the left liver lobe (arrow). (**b**) Axial T_1-weighted image (FLASH sequence, 110/9 ms, 80°) acquired after puncturing and injecting diluted paramagnetic contrast agent in the bile ducts of the left liver lobe. The needle (arrowhead) and the central tumor (T) are easily visualized. (**c – d**): Extracts from the continuously acquired (every 1.3 s) T_2-weighted image series (true FISP sequence, 12.5/5.9 ms, 80°) that controls guidewire insertion and catheter advancement. Artifact due to field inhomogneities (A). (**c**) Catheter tipp in the bile duct of the left liver lobe, wire tipp (arrow) within the catheter (arrowhead). (**d**) tipp of the guidewire (arrow) and catheter in the central bile ducts, (**e**) Conventional cholangiography acquired after MRI-guided catheter insertion. Compression of the proximal common bile duct, contrast agent within the dilated bile ducts of the left liver lobe (arrow), the distal common bile duct (B), and the duodenum.

during continuous image acquisition using the true FISP sequence (Fig. **1 c – d**). After safe catheter positioning in the bile ducts, in all patients three attempts were made to advance the guide wire and catheter past the obstruction under MRI control. The final catheter position was documented with the above-mentioned FLASH sequence. After experiment completion in MRI, catheter position in all patients was fluoroscopically controlled by injecting a radiocontrast agent (Imeron 300, Byk-Gulden, Konstanz) (Fig. **1 e**). Under fluoroscopy, three further attempts were made to pass the biliary obstruction.

Evaluation

The time duration of the interventions was determined. The total procedure time was measured, beginning with the initial puncture-needle contact with the patient's skin and ending with final catheter placement. Within this total time period, puncture duration itself was measured, beginning with the initial contact of the puncture needle with the patient's skin and ending with evidence of bile reflux; puncture including wire insertion ended with guide-wire visualization in the contrast-enhanced bile ducts. The procedure time of catheter manipulations was measured from the first insertion of the catheter to its final placement including the three attempts to pass the obstruction. Additionally, for the MRI-guided interventions, we measured the time duration of the pre-interventional imaging including target-plane determination, beginning with localizer acquisition and ending with visualization and marking of the puncture location on the skin. All patients filled out a questionnaire 48 h after intervention regarding their subjective experience of the intervention. Complications occurring up to 48 h after intervention were recorded as being intervention related.

Results

The MRC which visualized the dilated first and second order bile ducts, and the T_1-weighted axial tomographs facilitated planning of the percutaneous access to the biliary tract in all patients (Fig. **1 a**).

The near-real-time visualization aided by the T_2-weighted true FISP sequence allowed the successful puncture of the dilated bile ducts in three patients in the first attempt; in two patients a second and in one a third puncture attempt had to be made after retracting the needle, because the initial puncture attempts failed. The average time needed for the MRI-guided punctures was 164 ± 139 s. The image quality of the true FISP sequence was somewhat reduced by inhomogeneity artifacts (Abb. **1**c); this interfered with the correct positioning of the needle and catheter in one patient. To position the catheter in bile ducts whose curved anatomy deviated from the image plane, continuous acquisition of 3 slices was necessary, which were modified to follow the course of the bile ducts in order to track the catheter without interruption. The catheter tipp could be delimited due to its Cobra configuration (Fig. **1 c**) and clearly localized once the guide wire was inserted (Fig. **1 d**). The time duration for the MRI-guided catheter manipulations varied considerably from 10:56 min. to 29:20 min. (average 20:12 ± 6:13 min.) depending on the given anatomy. The final catheter position was precisely visualized in all cases by MRI in comparison with the results obtained by fluoroscopy (Fig. **1 d, e**). Under MR guidance, wire or catheter passing of the obstruction was unsuccessful in all patients; immediate attempts at passage under fluoroscopy led to success in one patient.

Fluoroscopy-guided puncture was successful in 1 patient on the first attempt, in 3 patients on the second attempt, and in one patient each on the third and fifth attempts. In 2 patients the obstruction could be passed. The other patients received an external drainage. The average time duration for puncture and catheter manipulation is shown in Table **1**.

Table 1: Average time required for biliary tract drainage (n = 12). The total time includes puncture, catheter manipulation, and bile-duct visualization.

	Bile duct drainage	
MRC and localization	10:47 ± 2:35 min.	
Puncture	2:44 ± 2:19 min.	3:31 ± 1:58 min.
contrast injection and guide-wire insertion	8:02 ± 2:03 min.	4:53 ± 2:43 min.
catheter manipulation	20:12 ± 6:13 min.	10:53 ± 3:55 min.
total	46:08 ± 10:21 min.	21:48 ± 8:33 min.

Patient acceptance was higher for the fluoroscopic procedure than for the MR-guided interventions. According to the the questionnaire, the longer mean intervention time of the MRI procedures was primarily responsible for this result. There were no serious complications requiring intensive medical attention in the two groups.

Discussion

MRI allows a precise, non-invasive planning of a biliary intervention based on MRC in an open low field system [7,8,11]. Moreover, the technique of susceptibility-based needle and catheter tracking introduced here facilitated the targeted puncture of the bile ducts under MRI control in an open MR system; external bile drainage was successful in all patients. Passing the obstructions failed in all of our patients. This might be accomplished given further mechanical improvements, especially of the guide wire. It should be noted that, directly after MRI-guided catheter placement, passing the central obstruction under fluoroscopy succeeded in only one patient.

Clinical application of the methods introduced here appears useful in cases requiring high accuracy because MRC facilitates optimal planning and the patient does not have to be repositioned for the targeted puncture and the external drainage procedure. Indeed, the puncture time in the present study was even faster than under fluoroscopic guidance. Furthermore, the frequently high radiation exposure of the examiner's hands associated with fluoroscopy-guided biliary interventions is avoided [14,15].

Catheter tracking under MRI control also showed acceptable results due to the use of a catheter prototype whose material composition makes it visible in the MR image. This catheter obviates the application of MRI-visible markers [9] as well as a wire incorporated into the catheter that emits a direct artifact-inducing current [12]. Thus both the mechanical and biological

properties of the catheter prototype used in this study are not different from conventional angiography catheters. Catheters and guide wires are designed to induce a relatively large artifact which ensured distinct device visualization. To avoid signal interference of the wall structures [11], the artifact width can be modified to the given situation by changing the measurement sequences [9], or by using various catheters and guide wires producing different artifacts, although this was not necessary in our experiments. Combining the catheter with the guide wire, the former completely visible in the MR image and the latter visible only at its tip, proved efficacious. Similar catheter-wire combinations have also been introduced in angiography.

A substantial drawback of the MR-guided interventions – especially the susceptibility based catheter tracking – was their duration, which the patients also considered to be long. Despite the relatively straight course of the biliary tract, slice orientation usually has to be modified several times to the anatomic situation. However, changing a given sequence parameter in our open MR system (e.g., slice orientation, number of slices, slice position) currently necessitates a complete reloading of the sequence. This considerably delays visualization. It also makes the monitoring of the guide wire and of catheter manipulations much more complicated and longer than is the case under fluoroscopy.

The disadvantages of susceptibility-based visualization may possibly be overcome by using active instrumentation tracking. This technique, however, requires extensive hard- and software modifications of the MRI [3, 7] and the use of active visualization with roadmapping may be very difficult in cases of target organs that shift during breathing, such as the liver. Here, near-real-time imaging is needed in addition to active tracking. With the image repetition rate of 1.3 seconds achieved in this study, at least 10 images per breath-hold were acquired; in the coronal orientation of the control planes the needle could be visualized in the target plane in each image even in cases of incomplete breath-hold. Nevertheless, the temporal resolution achieved up to now cannot yet compare with radiologic visualization, which was particularly clear when tracking the catheter.

In conclusion susceptibility-based MR visualization has the significant advantage of being applicable in every open MRI scanner without needing expensive device modifications. The method introduced here must be improved by further developing the instrumentation, by accelerating image acquisition, and by further modifying the MR system to the intervention requirements. It remains to be seen whether this simple and technically robust technique can be used for performing more complex MRI-guided endovascular interventions such as TIPS or tumor embolizations.

References

[1] Frahm C, Gehl HB, Weiss HD, Rossberg WA. Technik der MRT-gesteuerten Stanzbiopsie im Abdomen an einem offenen Niederfeldgerät: Durchführbarkeit und erste klinische Ergebnisse. Fortschr Geb Röntgenstr Neuen Bildgeb Verfahr 1996; 164: 62 – 67

[2] Lewin JS, Petersilge CA, Hatem SF, Duerk JL, Lenz G, Clampitt ME, Williams ML, Kaczynski KR, Lanzieri CF, Wise AL, Haaga JR. Interactive MR imaging-guided biopsy and aspiration with a modified clinical C-arm system. Am J Roentgenol 1998; 17: 1593 – 1601

[3] Steiner P, Schoenenberger AW, Penner EA, Erhart P, Debatin JF, von Schulthess GK, Kacl GM. Interaktive, stereotaktische Interventionen im supraleitenden, offenen 0.5-Tesla-MR-Tomographen. Fortschr Geb Rontgenstr Neuen Bildgeb Verfahr 1996; 165: 276 – 280

[4] Wacker FK, Cholewa D, Roggan A, Schilling A, Waldschmidt J, Wolf KJ. Vascular lesions in children: percutaneous MR imaging-guided interstitial Nd:YAG laser therapy-preliminary experience. Radiology 1998; 208: 789 – 794

[5] Reither K, Wacker F, Ritz JP, Isbert C, Germer CT, Roggan A, Wendt M, Wolf KJ. Laserinduzierte Thermotherapie (LITT) von Lebermetastasen in einem offenen 0,2T MRT. Fortschr Geb Röntgenstr Neuen Bildgeb Verfahr 2000; 172: 175 – 178

[6] Lu DS, Sinha S, Lucas J, Farahani K, Lufkin R, Lewin K. MR-guided percutaneous ethanol ablation of liver tissue in a 0.2-T open MR system: preliminary study in porcine model. J Magn Reson Imaging 1997; 7: 303 – 308

[7] Göhde SC, Pfammatter T, Steiner P, Erhart P, Romanowski BJ, Debatin JF. MR-guided cholecystostomy: assessment of biplanar, real-time needle tracking in three pigs. Cardiovasc Intervent Radiol 1997; 2: 295 – 299

[8] Wacker F, Branding G, Wagner A, Ewert A, Faiss S, Wendt M, Wolf KJ. MRT-gestützte Gallenwegsdrainage: Erprobung der passiven Katheterdarstellung an einem Tiermodell. Fortschr Geb Röntgenstr Neuen Bildgeb Verfahr 1998; 169: 649 – 654

[9] Bakker CJ, Hoogeveen RM, Hurtak WF, van Vaals JJ, Viergever MA, Mali WP. MR-guided endovascular interventions: susceptibility-based catheter and near-real-time imaging technique. Radiology 1997; 202: 273 – 276

[10] Manke C, Nitz WR, Lenhart M, Volk M, Geissler A, Djavidani B, Strotzer M, Kasprzak P, Feuerbach S, Link J. Stentangioplastie von Beckenarterienstenosen unter MRT-Kontrolle: Erste klinische Ergebnisse. Fortschr Geb Rontgenstr Neuen Bildgeb Verfahr 2000; 172: 92 – 97

[11] Wacker F, Branding G, Zimmer T, Faiss S, Wolf KJ. MR Cholangiopankreatikographie am offenen Niederfeldsystem: Erste klinische Ergebnisse im Vergleich zum Hochfeldsystem und zur ERCP. Fortschr Geb Röntgenstr Neuen Bildgeb Verfahr 1997; 167: 579 – 584

[12] Adam G, Glowinski A, Neuerburg J, Bücker A, van Vaals JJ, Hurtak W, Günther RW. Kathetervisualisierung in der MR-Tomographie: erste tierexperimentelle Erfahrungen mit Feldinhomogenitätskathetern. Fortschr Geb Röntgenstr Neuen Bildgeb Verfahr 1997; 166: 324 – 328

[13] Schild H, Klose KJ, Staritz M, Borner N, Nagel K, Günther R, Rückert K, Junginger T, Thelen M. Ergebnisse und Komplikationen von 616 perkutanen transhepatischen Gallenwegsdrainagen. Fortschr Geb Röntgenstr Neuen Bildgeb Verfahr 1989; 151: 289 – 293

[14] Krahe T, Ewen K, Lackner K, Koster O, Nicolas V. Die Strahlenexposition des Patienten und Untersuchers in der interventionellen Radiologie. Fortschr Geb Röntgenstr Neuen Bildgeb Verfahr 1986; 145: 217 – 220

[15] Williams JR. The interdependence of staff and patient doses in interventional radiology. Br J Radiol 1997; 7: 498 – 503

Frank Wacker MD

Department of Radiology
University Hospital Benjamin Franklin
Free University of Berlin
Hindenburgdamm 30, 12200 Berlin
Germany

Tel. + 49.30.84453041
Fax + 49.30.84454474
E-mail: wacker@ukbf.fu-berlin.de